REPORT DOCUMENTATION PAGE

Form Approved
OMB No. 0704-0188

AD-A265 729

...tion is estimated to average 1 hour per response, including the time for reviewing instructions, searching existing data sources, ...pleting and reviewing the collection of information. Send comments regarding this burden estimate or any other aspect of this ...educing this burden, to Washington Headquarters Services, Directorate for information Operations and Reports, 1215 Jefferson ... 2, and to the Office of Management and Budget, Paperwork Reduction Project (0704-0188), Washington, DC 20503.

2. REPORT DATE	3. REPORT TYPE AND DATES COVERED
May 12, 1993	Technical Report / June 1992-May 1993

4. TITLE AND SUBTITLE
Kinetics of Mediated Electron Transfer between Viologen Groups in a Self-Assembled Monolayer and Metal Complexes in Solution

5. FUNDING NUMBERS
Grant # N00014-90-J-1167
R&T Code 4133019

6. AUTHOR(S)
THomas Schneider, Shauna Hiley, and Daniel A. Buttry

7. PERFORMING ORGANIZATION NAME(S) AND ADDRESS(ES)
Department of Chemistry, University of Wyoming
Laramie, WY 82071-3838

8. PERFORMING ORGANIZATION REPORT NUMBER

DTIC ELECTE JUN 14 1993 S D

9. SPONSORING/MONITORING AGENCY NAME(S) AND ADDRESS(ES)
Office of Naval Research
Chemistry Division
800 N. Quincy Street
Arlington, VA

10. SPONSORING/MONITORING AGENCY REPORT NUMBER
Technical Report #21

11. SUPPLEMENTARY NOTES
Prepared for publication in Journal of the American Chemical Society

12a. DISTRIBUTION/AVAILABILITY STATEMENT
This document has been approved for public release and sale; its distribution is unlimited

12b. DISTRIBUTION CODE

13. ABSTRACT *(Maximum 200 words)*

Self-assembled monolayers are used in an experimental configuration which allows the extraction of the cross reaction electron exchange rate constant for the electron transfer between a viologen group embedded within the SAM and a metal complex in solution. This cross reaction rate constant is compared with predictions from the Marcus theory using the cross reaction relation and the known self-exchange rate constants for the two reagents. The results reveal that the intrinsic barrier to the electron transfer is relatively unchanged in the SAM, while the rate constant is somewhat depressed due to the long distance over which the electron must transfer.

93-13170

93 [illegible] 005

14. SUBJECT TERMS
electrochemistry, Marcus theory, cross reaction

15. NUMBER OF PAGES
28

16. PRICE CODE

17. SECURITY CLASSIFICATION OF REPORT	18. SECURITY CLASSIFICATION OF THIS PAGE	19. SECURITY CLASSIFICATION OF ABSTRACT	20. LIMITATION OF ABSTRACT
unclassified	unclassified	unclassified	UL

OFFICE OF NAVAL RESEARCH

Grant # N00014-90-J-1167

R&T Code 4133019

Technical Report #21

Kinetics of Mediated Electron Transfer between Viologen Groups in a Self-Assembled Monolayer and Metal Complexes in Solution

by

Thomas Schneider, Shauna Hiley, and Daniel A. Buttry

Prepared for Publication in

Journal of the American Chemical Society

Department of Chemistry
University of Wyoming
Laramie, WY 82071-3838

May 12, 1993

Reproduction in whole or in part is permitted for any purpose of the United States Government.

This document has been approved for public release and sale; its distribution is unlimited.

KINETICS OF MEDIATED ELECTRON TRANSFER BETWEEN VIOLOGEN GROUPS IN A SELF-ASSEMBLED MONOLAYER AND METAL COMPLEXES IN SOLUTION

Thomas Schneider, Shauna Hiley, and Daniel A. Buttry*
Department of Chemistry
University of Wyoming
Laramie, WY 82071-3838

Abstract

The kinetics of the thermodynamically downhill outer-sphere electron transfer between viologen redox groups embedded within several different types of self-assembled monolayers (SAM's) on Au electrodes and $Ru(NH_3)_6^{3+}$ in solution are examined. These cationic SAM's are shown to be very good barriers for blocking direct access of the cationic metal complex to the underlying electrode, thus forcing electron exchange between the metal complex and the electrode to occur by virtue of mediation through the viologen redox groups. This allows measurement of the rate constant for the electron exchange cross reaction (k_{crs}) between the one-electron reduced form of the embedded viologen (V^+) and $Ru(NH_3)_6^{3+}$. When the viologen redox group is "buried" within the SAM (i.e. has an alkyl or fluorocarbon chain or a cholesteryl moiety between it and the solution), the observed cross reaction rate constants seem to be primarily influenced by the degree of defectiveness of the monolayer, making quantitative discussion of the rate constants difficult. For the case of a SAM which has a pendent viologen group directly exposed to the solution (i.e. present at the monolayer/solution interface rather than "buried" within the hydrocarbon layer of the SAM), the system is more well-behaved, making it possible to give a quantitative comparison between the experimentally observed rate constant, k_{crs}, and that calculated from Marcus theory using the known values of the self-exchange rate constants for these two redox couples, $k_{crs,th}$. These values are: $k_{crs} = 1 \times 10^5\ M^{-1}\ s^{-1}$ and $k_{crs,th} = 1 \times 10^7\ M^{-1}\ s^{-1}$. The rather large difference between these values is primarily attributed to a distance dependence of the electron transfer rate constant for the SAM system due to the presence of a methyl group intervening between the viologen redox group in the SAM and the ruthenium complex in solution. Other possible origins of the depressed rate in the SAM are also discussed. To our knowledge, this study represents the first application of Marcus theory to electron exchange cross reactions in monolayer systems.

A-1

Introduction

One of the driving forces for the large and growing body of work on self-assembled monolayers (SAM's) (1) is their potential for use in studies of electron transfer kinetics at highly structured interfaces. Several groups have applied SAM technology to this problem. For example, Chidsey (2) and Finklea and coworkers (3) have both used SAM methodology to produce interfacial structures in which redox groups are held at fixed distances from the electrode surface, thereby allowing for the determination of electron transfer rate constants at well-defined distances and/or as a function of distance. These elegant experiments are especially relevant given the high degree of current interest in understanding those factors which influence the rates of long range electron transfer (4).

Our group has developed a series of self-assembling viologen derivatives which bear thiol or disulfide functionalities at the ends of long alkyl chains. These functionalities allow for these molecules to be covalently anchored to Au and Ag surfaces to form stable SAM's which are essentially irreversibly adsorbed. These SAM structures have been used to address questions related to the coupling between ionic motion in and out of the monolayer and the transfer of electrons between the redox groups in the monolayer and the underlying electrode (5), as well as the influence of the position of the redox group within the monolayer structure on its redox properties (6). As part of a continuing effort to understand interfacial electron transfer in such systems, we describe here a series of experiments in which these viologen derivatives are used as mediators to transfer electrons between the underlying electrode and redox couples present in solution. As will be discussed further below, the experimental conditions employed allow one to extract the rate constant for the electron exchange cross reaction between the viologen group (embedded in the SAM) and the redox species in solution. Comparison of these experimentally obtained rate constants with theoretical predictions from Marcus theory reveals that cross reaction which occurs in these self-assembled monolayers is essentially the same as that which would occur in solution.

Experimental

All chemicals used in synthesis and electrochemical experiments were of reagent grade or better. Water was purified by a Millipore purification train and was used for all electrolyte solutions.

Synthesis:

All of the derivatives were synthesized according to the general route shown in Scheme 1. The methyl terminated derivatives (vide infra) were all prepared as thiols, while the other derivatives were prepared as dislufides. Significant differences in behavior were observed for these two types of anchoring groups which will be discussed in a future publication.

N-(methyl)-N'-(10-mercaptodecyl)-4,4'-bipyrdinium iodide bromide (1V10SH) was synthesized by the following precedure. Methyl iodide was reacted with 4,4'-dipyridyl in a 0.9 to 1 ratio for 3 hours in acetone at reflux. The precipitate was collected and washed with acetone 3 times to remove unreacted starting materials. NMR revealed pure N-(methyl)-4,4'-bipyridinium iodide. The second alkyl chain was attached by dissolving this product in DMF and reacting it with a 1:1 molar ratio of 10-bromo-1-decyl thioacetate for 36 hours near reflux. The precipatate was collected, washed 3 times with acetonitrile, and characterized by NMR. The thioacetate was cleaved to the thiol by dissolving in 50 mL of dry, cold, degassed methanol, then adding 5 mL of acetyl chloride. While stirring, the solution was allowed to warm to room temperature for 3 hours under N_2 purge. The solid was isolated by evaporation of the solvent and other materials.

N-(methyl)-N'-(12-mercaptododecyl)-4,4'-bipyridinium iodide bromide (1V12SH) was prepared in a similar manner to 1V10SH, using 12-bromo-1-dodecyl thioacetate rather than 10-bromo-1-decyl thioacetate.

N-(methyl)-N'-(16-mercaptohexadecyl)-4,4'-bipyridinium iodide bromide (1V16SH) was prepared in a similar manner to 1V10SH.

Bis[N-(n-decyl)-N'-(10-mercaptodecyl)-4,4'-bypridinium] disulfide dibromide $(10V10S\text{-})_2$ was prepared as previously reported (5).

Bis[N-(cholesteryl)-N'-(5-mercaptopentyl)-4,4'bipyridium] disulfide tosylate iodide $(ChoV5S\text{-})_2$ Cholesteryl p-toluene sulfonate (Sigma Chemical) was reacted with 4,4'-dipyridyl at a 0.8 to 1.0 molar ratio in a minimal amount of a 50/50 mixture of acetone and acetonitrile. After refluxing for 48 h the precipitate was filtered and rinsed with acetone. NMR revealed pure product (N-(cholesteryl)-4,4'-bipyridinium p-toluene sulfonate). Attachment of the second alkyl chain was achieved by reaction with a five molar excess of 1,5-diiodopentane for 2 days under nitrogen in DMF. The solvent was removed and the

product was washed with ether to remove excess 1,5-diiodopentane. Production of the thiouronium salt was achieved by reaction with a 5 molar excess of thiourea in DMF under nitrogen for 3 days. Solvent was again removed and the product's structure and purity were characterized by NMR. Cleavage of the thiouronium salt to produce the thiol was achieved by reaction with a 3:1 molar excess of Proton Sponge (Aldrich Chemical) in DMF under nitrogen. After 3.5 hours, 10% HCl was added dropwise until a pH of 4.0 was obtained. Solvent was then removed leaving the ChoV5SH and excess Proton Sponge which was extracted by washing with 1% HCL 3 times.

Bis[N-(n-1H,1H,2H,2H-perfluorododecyl)-N'-(5-mercaptopentyl)-4, 4'-bipyridinium] disulfide diiodide (F10H2V5S-)$_2$ was prepared by the following procedure. 1-iodo-1H,1H,2H,2H-perfluorododecane (PCR) was reacted at reflux with 4,4'-dipyridyl at a 1.0 to 1.0 molar ratio in acetone. After 3 days the precipitate was filtered and purified by Soxhlet extraction with high boiling petroleum ether. NMR revealed a pure product (N-(n-1H,1H,2H,2H-perfluorododecyl)-4,4'-bipyridinium iodide). Attachment of the second alkyl chain was achieved by reaction with a 5 molar excess of 1,5-diiodopentane in acetonitrile for 24 h. The precipitate was collected and washed with acetonitrile. NMR revealed pure product. The thiouronium salt was prepared by reacting this material with a 5 molar excess of thiourea in DMF under nitrogen for 24 h, after which the solvent was removed. The product was washed with acetone 3 times to remove excess thiourea and characterized by NMR. The thiouronium salt was cleaved to produce the thiol by stirring and modest heating in ethanol for 4 hours with a slightly less than 1 molar ratio of bicarbonate. Upon cooling the thiol precipitated and was collected and washed with cold ethanol.

Electrochemical measurements were made using a locally built potentiostat with an analog ramp generator or a BAS 1000. A standard H-cell was used for all electrochemical experiments and cleaned in hot nitric acid for 12 h prior to use. A SSCE was used as the reference electrode, to which all potentials are referenced. The counter electrode was a platinum wire. The thin film gold working electrodes (with geometrical areas of 0.34 cm^2) were prepared by vapor deposition onto quartz substrates (AT-cut, chemically polished single crystal quartz wafers from Valpey-Fisher). Prior to Au deposition, an adhesion layer of 3-mercaptopropyl trimethoxysilane was deposited onto the quartz surface, using the method described by Majda (7). These Au electrodes had an effective surface roughness of 1.2 measured by iodine chemisorption (8). All calculations of surface coverage are corrected for this surface roughness. The use of AT-cut quartz substrates for electrode preparation allowed

the use of an electrochemical quartz crystal microbalance (EQCM) to simultaneously monitor electrochemical processes and mass changes at the electrode surface. The instrumentation used for this has been described elsewhere, as have the considerations pertaining to its use to measure mass changes in monolayer samples (9). Solutions were thoroughly purged with Ar prior to the electrochemical measurements. This was especially critical in the present study due to the rapidity of the reaction between oxygen and V^+.

The following proceedure was used to prepare stable, self-assembled monolayers of these compounds. A saturated solution of the viologen was prepared in either methanol or ethanol. One or two drops of this saturated solution were added to 10 to 15 ml of 0.1 M NaCl electrolyte. To periodically (ca. every 3-5 hours) assay the surface coverage using cyclic voltammetry, the coating solution was removed and the monolayer was rinsed with 95% ethanol prior to transfer to a solution of pure supporting electrolyte. Typical coating times ranged from 2 to 24 h. Following this coating procedure, the SAM's were exposed to an ethanol solution containing a straight chain alkyl thiol of the appropriate length to "seal" the inner alkyl chain region of the monolayer, thereby preventing penetration of the solution phase redox reagent through the monolayer to gain direct access to the electrode. The length of this alkyl thiol was chosen so as to match the length of the inner chain of the viologen derivative (e.g. dodecane thiol to "seal" the 1V12SH monolayer). This process has been shown to produce high quality SAM's which can be used to hold pendent redox groups at well-defined distances from the underlying electrode surface (2,3). However, in the present case its sole purpose is to prevent direct communication between the electrode and the solution phase redox reagent, thereby forcing electron exchange between the solution phase redox couple and the electrode to occur by virtue of mediation through the viologen redox moieties within the SAM. This set of procedures was found to give fairly reproducible surface coverages which are near the saturation limit, based on parallel orientation of the long axis of the viologen ring system with respect to the surface normal. This orientation is consistent with the observed surface coverages and projected geometrical area of the viologen in the "end on" orientation. It is also in agreement with spectroscopic determinations of orientation based on the surface selection rules using infrared reflection absorption spectroscopy and surface enhanced Raman spectroscopy (10).

Results and Discussion

A. Kinetic Model

These viologen SAM's have previously been demonstrated to exhibit the

well-defined, chemically and electrochemically reversible redox responses of the viologen redox moiety (5,6), as represented by the following equation:

$$V^{2+} + e^- \text{ <----> } V^+ + e^- \text{ <----> } V^0 \quad (1)$$

where V^{2+} represents the fully oxidized form of the viologen group, V^+ the one-electron reduced form, and V^0 the fully reduced form. The exact potentials at which these redox processes occur depend on the nature of the counterion of the viologen group in the monolayer (5,6) and the position of the viologen group within the monolayer (6), but they fall in the range of -0.35 to -0.50 V for the first reduction and -0.70 to -0.90 V for the second reduction. For the purposes of the present discussion, we focus our attention on the first reduction, which produces the one-electron reduced cation radical, V^+. As will be demonstrated below, the electron exchange between V^+ and $Ru(NH_3)_6^{3+}$ is thermodynamically downhill by around 0.25 V, so that production of V^+ within the SAM (e.g. during a cyclic voltammetric (CV) experiment) in the presence of $Ru(NH_3)_6^{3+}$ in solution leads to electron exchange according to the following equation:

$$V^+ + Ru(NH_3)_6^{3+} \xrightarrow{k_{crs}} V^{2+} + Ru(NH_3)_6^{2+} \quad (2)$$

provided that the two reagents can gain access to one another and that the rate for the process is sufficient to allow its observation on the time scale of the CV experiment.

The electrochemical determination of k_{crs} for this situation is somewhat complicated by the possible influence of other kinetic processes on the overall rate of electron flow from the electrode, through the viologen SAM, and into the $Ru(NH_3)_6^{3+}$ redox reagent in solution. Figure 1 shows a diagram of the electrode/SAM/solution interfacial region along with schematic descriptions of these other processes, where k_s (with units of s^{-1}) represents the rate constant for the heterogeneous electron transfer between the electrode and the viologen redox group and k_{crs} (with units of $M^{-1}\ s^{-1}$) represents the rate constant for the electron transfer between V^+ and $Ru(NH_3)_6^{3+}$. Keeping in mind that an electrochemical determination of k_{crs} requires measurements of currents associated with passage of electrons between the electrode and $Ru(NH_3)_6^{3+}$ by virtue of mediation by the viologen redox group, we switch our attention to the currents for each of these processes, namely i_s and i_{crs}, respectively. These kinetic currents will bear the following relationship to the overall,

observed current, i_{obs}:

$$1/i_{obs} = 1/i_s + 1/i_{crs} \quad (3)$$

as is always observed for kinetic processes which occur in series. This relationship is similar to one previously used to evaluate cross reaction rate constants between polymer-bound redox couples and redox species in solution (11).

The following two equations give the *steady state* formulations of the two kinetic currents described above in equation 3. These formulations are quite useful in identifying those quantities which influence the two rate processes of interest. The two currents are given by:

$$i_s = n F A k_s \Gamma \quad (4)$$

$$i_{crs} = n F A k_{crs} \Gamma [Ru(NH_3)_6^{3+}] \quad (5)$$

where n is the number of electrons transferred (n=1 in the present cases), F is the Faraday constant, A is the electrode area, and Γ is the surface coverage of the viologen redox moiety. Consideration of these two equations suggests that there may be conditions under which either i_s or i_{crs} individually limit (and therefore can be equated with) the overall observed current. For example, at high concentrations of $Ru(NH_3)_6^{3+}$, small values of k_s, or large values of k_{crs}, the observed kinetic current will be limited by the heterogeneous electron transfer process, leading to the case in which $i_{obs} = i_s$. Conversely, at low concentrations of $Ru(NH_3)_6^{3+}$, large values of k_s, or small values of k_{crs}, the observed kinetic current will be limited by the cross reaction rate, leading to the case $i_{obs} = i_{crs}$. This latter case is of interest here, for it provides a direct measure of the rate constant for the cross reaction between the immobilized redox group and that in solution. The proper formulation of i_{crs} for a non-steady-state, CV experiment and the manner in which k_{crs} is extracted from the data will be presented below.

There is some uncertainty as to how anion motion in and out of the monolayer during these electron transfer events (5,6) will influence the apparent values of the rate constants, k_s and k_{crs}. We will return to this point below, but note for the moment that it has been shown (12) that under conditions in which ion motion is concerted with (or coupled to) electron

transfer reactions, the apparent rate constant for the electron exchange processes of interest can be influenced by the rate process associated with the anion motion.

B. Determination of k_S

The kinetic scheme discussed above makes it clear that in order to properly evaluate the situation which prevails under a given set of experimental conditions, it is necessary to have at least a qualitative estimate of the values of k_S for the SAM's used in the cross reaction experiments. Determination of these values of k_S for several SAM types was done using procedures similar to those previously employed by Chidsey (2), Finklea and coworkers (3), and Hong and Mallouk (13). The kinetic responses of the "sealed" SAM's were probed using rapid scan CV experiments, and the separations of the anodic ($E_{p,a}$) and cathodic ($E_{p,c}$) peak potentials as a function of scan rate were used to calculate the values of k_S. The theory for this method has been discussed by Laviron (14). For these experiments, since the value of k_S is of interest, there was no $Ru(NH_3)_6^{3+}$ present in solution.

Figure 2 shows an example of the increase in peak separation (for the first reduction) with increasing scan rate for 1V10SH, and Figure 3 shows a plot of $E_{p,a}$ and $E_{p,c}$ versus log υ, where υ is the scan rate in V s^{-1}, also for 1V10SH. Proper analysis (14) of these data gives the values of k_S for both the cathodic ($k_{S,c}$) and anodic ($k_{S,a}$) electron transfers, as well as the transfer coefficients for both directions (α and 1-α, respectively). These values are given in Table 1 for several different viologen SAM's. The transfer coefficients are clearly too small, a phenomenon which has been attributed to defectiveness in the monolayer (13,15). This makes the quantitative use of these rate constants for evaluation of the distance dependence (between electrode and redox group) of electron transfer rates problematic at best, and this type of analysis is not included here for that reason. Nevertheless, the values given in Table 1 are not unreasonable in comparison to those reported by Chidsey (2) and Finklea and coworkers (3) for ferrocene and a ruthenium pentaamine pyridine complex, respectively, immobilized at the exterior of alkyl thiol SAM's. Further, these data clearly show that the rate of transferring electrons from the electrode to the viologen redox groups within the SAM is quite fast, suggesting that conditions can be found in which the cross reaction rate constant limits the overall current.

C. Determination of k_{crs}

With at least a qualitative knowledge of the kinetic currents expected for the heterogeneous electron transfer reaction between the electrode and the viologen group

embedded within the SAM, we now proceed to measurements of the cross reaction rate constant. Figure 4 shows the consequences of adding $Ru(NH_3)_6Cl_3$ to the solution prior to a CV scan over the first reduction wave. There are several salient features of this figure. First, the difference in the formal potentials of these two redox couples (for $V^{2+/+}$, E^f = -0.45 V and for $Ru(NH_3)_6^{3+/2+}$, E^f = -0.20) is readily apparent, and indicates that the cross reaction between them should be downhill by 0.25 V in the present case. Second, in the presence of the viologen SAM, the lack of any discernible current at the potential at which $Ru(NH_3)_6^{3+}$ would be reduced at a bare electrode strongly suggests that this cationic metal complex cannot permeate the cationic SAM to gain direct access to the underlying electrode. Third, in the presence of $Ru(NH_3)_6^{3+}$ the reduction peak for the $V^{2+/+}$ couple is shifted to considerably more positive potentials than in the absence of $Ru(NH_3)_6^{3+}$, and it is also made completely irreversible. Taken together, these observations suggest that $Ru(NH_3)_6^{3+}$ is reduced by reaction with V^+ according to equation 2, and is not reduced by gaining electrons from the electrode directly.

The steady state kinetic treatment described above is quite straightforward, and should apply to the case of measurement of the kinetics for interfacial reactions using rotating disk voltammetry, as previously described by Anson (11b) and Murray and coworkers (11a,16). The simplicity of this steady state treatment prompted us to attempt to extract k_{crs} from rotating disk experiments. However, the monolayers were not sufficiently stable under these conditions to allow for reliable extraction of kinetic values from the experimental data. The instability seemed to be related to passage of large currents through the SAM during the mediation. Since the monolayers appeared more stable toward repeated CV experiments at more modest currents, an alternative procedure was employed for measuring k_{crs} which is based on a kinetic scheme originally developed by Andrieux and Saveant (17) for reaction between an immobilized catalyst and a redox reagent in solution. Their model, *which applies to potentiodynamic, not steady state, conditions*, is pertinent to the present case because all of the current which flows to $Ru(NH_3)_6^{3+}$ is mediated by the $V^{2+/+}$ couple, which, therefore, acts essentially as a redox catalyst. Basically, the model allows direct calculation of the apparent rate constant for the mediation process, k_{obs}, from the shift in the peak potential for the mediated wave during a CV experiment according to the following equation:

$$E_{p,med} = E^0_V - 0.78(RT/F) + (RT/F)\ln\{k_{obs}\Gamma/(D_{Ru}Fv/RT)^{1/2}\} \quad (6)$$

where $E_{p,med}$ is the peak potential for the mediated current, E^0_V is the formal potential for

the $V^{2+/+}$ redox couple, D_{Ru} is the diffusion coefficient of $Ru(NH_3)_6^{3+}$, and the other quantities have already been defined. Note that we identify the experimentally observed rate constant as k_{obs} because it could, in principle, contain contributions from k_{crs} and/or k_s.

The Andrieux/Saveant model also predicts that the observed peak current for a mediated electron transfer process, $i_{obs,p}$, will be given by:

$$i_{obs,p} = 0.496\ F\upsilon\ [Ru(NH_3)_6^{3+}]\ D_{Ru}^{1/2}\ (F\upsilon/RT)^{1/2} \qquad (7)$$

where the quantities are as before. This equation applies when the kinetically limiting current is i_{crs} (i.e. $i_s >> i_{crs}$, so $i_{obs} = i_{crs}$), meaning that the electrode reaction can reduce the pendent viologen groups much faster than they are oxidized by the $Ru(NH_3)_6^{3+}$ which is delivered to the surface by diffusion from solution. The equation shows that the current peak behaves as for a diffusion process, depending on the square root of scan rate, the concentration of the solution phase redox couple, and the square root of its diffusion coefficient. On the other hand, under conditions where the observed current is limited by the inner electron exchange (i.e. between the electrode and the bound viologen redox couple), the peak current should depend on the first power of scan rate, and have no dependence on either the concentration or diffusion coefficient of $Ru(NH_3)_6^{3+}$. Given that the two possible kinetically limiting currents are related as in equation 3, these considerations suggest that a plot of $1/i_{obs,p}$ versus $1/[Ru(NH_3)_6^{3+}]$ (at a constant scan rate) should be linear, with a slope of $(0.496\ F\upsilon\ D_{Ru}^{1/2}\ (F\upsilon/RT)^{1/2})^{-1}$. The intercept of the linear portion of the plot should give $i_{s,p}$, the peak current for the i_s process at that scan rate.

Figure 5 contains a plot of $1/i_{obs,p}$ versus $1/[Ru(NH_3)_6^{3+}]$. The plot clearly shows a non-zero slope, from which a value of $D_{Ru} = 1.9 \times 10^{-6}$ cm^2 s^{-1} can be extracted. This is essentially identical to the value of 2.1×10^{-6} cm^2 s^{-1} which was independently determined from potential step chronoamperometric experiments. The linearity of the plot and the very good agreement between these two values of D_{Ru} argue compellingly that, under the conditions of the experiments in Figure 5, the kinetically limiting current is i_{crs}.

Another test of the relative magnitudes of i_s and i_{crs} is based on whether the inner electron exchange rate process is capable of maintaining all of the viologen redox groups embedded within the SAM in the reduced form throughout the mediation process. Since previous electrochemical quartz crystal microbalance (EQCM) studies have demonstrated

that charge compensating anion expulsion accompanies the reduction of V^{2+} to V^{+} in these systems (5,6), this suggests that one way of addressing this question is to determine the change in anion population of the SAM during the reduction process in the presence and absence of $Ru(NH_3)_6^{3+}$ using the EQCM. Figure 6 shows EQCM results of three separate CV experiments conducted without $Ru(NH_3)_6^{3+}$ present (curve A), at a low concentration of $Ru(NH_3)_6^{3+}$ (curve B), and at a high concentration of $Ru(NH_3)_6^{3+}$ (curve C). These results clearly demonstrate that a net mass loss (frequency increase) occurs during and throughout the reduction process, with this mass loss being attributed to anion expulsion. The magnitude of this mass loss is the same in curves A and B, indicating that the number of anions lost is the same in these two cases. This strongly suggests that essentially all of the viologen redox groups are maintained in the one-electron reduced state during the mediation process (at low $[Ru(NH_3)_6^{3+}]$), implying that the inner electron exchange process is kinetically capable of supplying electrons faster than they are consumed by the outer cross reaction. On the other hand, at the higher $Ru(NH_3)_6^{3+}$ concentration used in curve C, the EQCM results reveal that less anions have been expelled during the reduction process. This is because a fraction of the population remains in the V^{2+} state during this scan. This fraction retains its anions, leading to a net mass loss (anion expulsion) which is smaller than those in curves A and B. This suggests that at this higher $[Ru(NH_3)_6^{3+}]$, the inner electron exchange process is no longer capable of supplying electrons fast enough to maintain all of the viologen redox groups in the reduced form, leading to simultaneous coexistence of V^{2+} and V^{+} within the SAM even at potentials where there would be no V^{2+} in the absence of $Ru(NH_3)_6^{3+}$. Thus, as the concentration of $Ru(NH_3)_6^{3+}$ is increased, kinetic control of the current is delivered to the inner electron exchange process, as predicted by Equations 3-5, with the relative populations of V^{2+} and V^{+} being determined by the relative magnitudes of i_S and i_{crs}. These results are quite interesting in that they show how it is possible to diagnose the kinetic situation which prevails under a given set of conditions by using the EQCM to monitor the steady state populations of various species at the electrode surface.

These EQCM results and the plot in Figure 5 constitute clear evidence that i_S is larger than i_{crs} at concentrations of $Ru(NH_3)_6^{3+}$ in the range of 0.1 - 5.0 mM and scan rates near 50 mV s^{-1}. This implies that the observed kinetic currents can be used to calculate k_{crs} in that range of concentrations, so long as the peak current can be shown to depend in the proper way on $[Ru(NH_3)_6^{3+}]$ and scan rate. Thus, k_{crs} values for all of the SAM's studied were obtained from peak shifts at a $[Ru(NH_3)_6^{3+}]$ of 0.5 mM and scan rate of 50 mV s^{-1}, and are reported in Table 2, along with the surface coverages of the viologen groups in the "sealed"

SAM's, their formal potentials, and the peak potentials of the mediated waves. Note that these cross reaction rate constants have units of M^{-1} s^{-1} as is appropriate for second order rate constants.

We return to a discussion of the relative values of these cross reaction rate constants below, but first it is useful to place these values in context with expectations derived from the Marcus cross reaction relation. Thus, for the methyl terminated 1V10SH SAM a Marcus theory estimate of the predicted solution phase cross reaction rate constant, $k_{crs,th}$ (also given in Table 2), was calculated using the following relationships (18):

$$k_{crs,th} = (k_{11}k_{22}K_{12}f_{12})^{1/2} \qquad (8)$$

where k_{11} is the self-exchange rate constant for the $Ru(NH_3)_6^{3+/2+}$ couple (taken as 4×10^3 M^{-1} s^{-1} (19)), k_{22} is the self-exchange rate constant for the $V^{2+/1+}$ couple (taken as 8×10^6 M^{-1} s^{-1} (20)), K_{12} is the equilibrium constant for the process (calculated from the difference in formal potentials of $Ru(NH_3)_6^{3+}$ and the embedded viologen group of 0.25 V), and f_{12} is given by (18):

$$\log f_{12} = (\log K_{12})^2 / 4 \log (k_{11}k_{22}/Z_{homo}^2) \qquad (9)$$

where Z_{homo} is the homogeneous collision frequency (taken to be 10^{11} M^{-1} s^{-1}). Use of the appropriate values in equations 8 and 9 predicts a value of $k_{crs,th}$ of 1×10^7 M^{-1} s^{-1}. Note that this calculation uses the reported *solution phase* self-exchange rate constants, but a driving force calculated from the difference in redox potentials between the ruthenium complex in solution and the viologen group *in the SAM*. Since the viologen redox potential in solution (estimated from the formal potential of dissolved dimethyl viologen of -0.71 V) is so much more negative, use of these relationships to estimate the cross reaction rate constant *in solution* gives a value of 4×10^8 M^{-1} s^{-1}, considerably larger than the SAM estimate.

The value of 10^7 M^{-1} s^{-1} calculated for $k_{crs,th}$ for the SAM cross reaction is considerably larger than any of the experimental k_{crs} values given in Table 2, which range between 10^4 M^{-1} s^{-1} for the SAM's with viologen groups embedded within the monolayer and 10^5 M^{-1} s^{-1} for those which are methyl terminated, thereby placing the viologen group nearer to the SAM/solution interface. That $k_{crs,th}$ is so much larger than the k_{crs} values for the buried SAM's is probably due to an inability of the $Ru(NH_3)_6^{3+}$ complex to closely

approach the buried viologen group because of the steric constraints imposed by the alkyl or perfluoroalkyl chains. This will lead to a small cross reaction rate constant because of the very strong distance dependence of electron transfer rates (2-4). (As an aside, these data suggest that it may be possible to use results of this type to determine the distance dependence of these cross reaction rates, a topic which we are exploring.) An exception to this behavior for the embedded cases is presented by the derivative bearing a cholesteryl group at the SAM/solution interface. For this molecule, the cross reaction rate constant appears to be quite high. However, we have reason to believe that the monolayers formed form this species are highly defective, thereby allowing reasonably direct access of $Ru(NH_3)_6^{3+}$ to the viologen group. Kaifer and coworkers (21) have recently reported on similarly defective monolayers formed by reversible adsorption of (non-covalently anchored) viologen derivatives bearing terminal cholesteryl groups, a finding which corroborates this.

In contrast to the cases in which the viologen group is embedded within the SAM, the data for the 1V10SH, 1V12SH, and 1V16SH SAM's should be more comparable to the rate constant predicted by Marcus theory, given that $Ru(NH_3)_6^{3+}$ can approach the viologen redox group within the SAM much more closely. However, in spite of this, the k_{crs} values for all three of these SAM's are uniformly about two orders of magnitude below $k_{crs,th}$. This large difference between the predicted and observed values for the cross reaction rate constants for the three methyl terminated systems could have several possible origins. First, it is possible that the k_s values are, in fact, not large enough to be neglected in the kinetic analysis, and are limiting the observed kinetic currents. However, this is unlikely given the dependence of the observed kinetic currents on $[Ru(NH_3)_6^{3+}]$ as shown in Figure 5, and the EQCM results. Second, it is possible that the electrostatic work done in bringing $Ru(NH_3)_6^{3+}$ up to the surface prior to reduction is depressing the apparent rate constant, in what would essentially be a kinetic double layer correction for the monolayer system (22). However, we have explored the dependence of the apparent rates on ionic strength, and find no dependence in the range 0.1 to 1.0 M, indicating that work terms are not important at the 0.1 M ionic strengths used for these kinetics experiments. Further, past EQCM studies of these viologen SAM systems indicate that essentially all of the immobilized viologen groups are electrostatically neutralized by virtue of the presence of charge compensating anions within the monolayer. Thus, it seems intuitively reasonable that this charge compensation (which behaves, in the extreme, as ion-pairing (5)) would serve to screen out electrostatic repulsion between $Ru(NH_3)_6^{3+}$ and the surface bound viologen groups, thereby minimizing or even eliminating any electrostatic work associated with bringing $Ru(NH_3)_6^{3+}$ up to the

surface. Third, it is possible that the outer sphere reorganization energies which are almost certain to dominate the rate constants in the solution self-exchange cases may be considerably different in the SAM than in solution, which might lead to a rate depression relative to the solution case. Fourth, there could be subtle distance and/or orientational effects for the SAM cross reaction which jointly conspire to depress the rate constant below the Marcus value. Fifth, it is possible that the cross reaction electron transfer event requires simultaneous motion of ions into or out of the monolayer. In such a situation, the value of k_{crs} might be influenced by the rate constant for the ion motion (12) as discussed above, leading to an apparent value of k_{crs} which is not predictable by the Marcus relations.

There are several considerations relevant to the discussion of the rate of ion motion at this point. First, EQCM measurements on these SAM's in absence of redox couples in solution have consistently demonstrated that anion expulsion is coupled to the injection of electrons into the monolayer (and vice versa) to maintain charge compensation within the monolayer. Figure 6 shows that this also occurs during mediation. While these results do not speak directly to the issue of the possible influence of ion motion on k_{crs}, they do suggest the possibility that anion insertion into the SAM is *transiently* required in order for the cross reaction process shown in equation 2 to occur. If this is true, then the coupling of anion insertion with the cross reaction might lead to a dependence of k_{crs} on the rate constant for the ion motion process. A problem with this interpretation is that anion insertion and expulsion must also occur during the rapid scan CV experiments designed to elucidate the values of k_s for these SAM's, yet the k_s values obtained in these rapid scan experiments imply much larger rates for the inner (k_s) than the outer (k_{crs}) electron transfer processes. These results speak strongly against anion motion as being rate limiting for the cross reaction. Second, given that the inner electron transfer rate appears to be so large for these SAM's it does not seem unreasonable to speculate that transient charge compensation during the cross reaction could be achieved by electron transfer from the electrode to the viologen redox group rather than anion motion. In this case, there would be no influence of ion motion on k_{crs}. Thus, in the absence of any data directly linking ion motion to the observed rate constants, we favor the other possibilities discussed above as candidates for the cause of the relative rate depression in the SAM's.

We consider now the distance and/or orientation dependence argument. Given that the predicted solution phase cross reaction rate constant is well below the diffusion controlled value of ca. 10^{11} M^{-1} s^{-1}, it is anticipated that *in solution* the two reaction partners are able

to freely sample a wide range of possible orientations prior to the actual electron transfer event. Thus, during the many collisions which would take place in a particular encounter between $Ru(NH_3)_6^{3+}$ and V^+, the metal complex would likely find itself gaining direct access to the ring system of the viologen species several times. However, in the SAM cross reaction experiment the ruthenium complex is constrained to approach only as close as will be allowed by van der Waals contact with the terminal methyl group of the viologen derivative, a distance of ca. 4-5 Å (23). If the solution phase cross reaction rate constant pertains to the case of closest contact of the ruthenium complex directly with the aromatic ring system, then we can estimate the predicted change in the rate constant caused by the interposition of the methyl group in the traditional way using (3,4,18):

$$k = k_o e^{-\beta r} \qquad (10)$$

where k_o is the rate constant at closest contact (i.e. the cross reaction rate constant predicted above using the Marcus cross reaction relation, Equation 8), k is the rate constant at some farther distance, r, and β is a decay constant. For non-protein systems with covalently linked spacers, β is in the range of ca. 0.7 - 0.9 $Å^{-1}$ (4). Using the ranges of values for β and r and taking $k_o = 1 \times 10^7\ M^{-1}\ s^{-1}$, one arrives at a range of values for k of $(1 - 6) \times 10^5\ M^{-1}\ s^{-1}$. Thus, this distance dependence correction seems to account for nearly all of the discrepancy between k_{crs} and $k_{crs,th}$. Given the typical accuracy of rate constant measurements of this type (ca. a factor of 2) and the level of agreement between theory and experiment generally obtained by Marcus theory calculations (within an order of magnitude), additional discussion of remaining discrepancies would seem inappropriate.

Conclusions

While outer-sphere electron mediation from redox groups within adsorbed monolayers to solution phase redox reagents has been reported previously (21,24), to our knowledge this study represents the first detailed application of Marcus theory to electron exchange cross reaction kinetics in monolayer systems. This study has demonstrated that, by judicious choice of reaction conditions and careful construction of the appropriate SAM system, it is possible to extract electron exchange cross reaction rate constants from relatively straightforward electrochemical measurements. Further, in the present case, these rate constants compare very favorably with those predicted using the Marcus cross reaction relation (18). Thus, the methods described here should be of general value in determining cross reaction rate constants for a fairly wide variety of redox reagents, given that one of the

reaction partners can be immobilized within an appropriate SAM structure.

Given the wide applicability of the kinetic approach described here, it is worthwhile examining the range of rate constants which can be extracted from such an analysis. This is most easily done by converting the cross reaction rate constant, k_{crs}, into an *effective* heterogeneous electron transfer rate constant, $k_{s,eff}$, by multiplying it times the viologen redox group surface coverage, Γ (11a):

$$k_{s,eff}\,(\text{cm s}^{-1}) = k_{crs}\,(\text{cm}^3\,\text{mol}^{-1}\,\text{s}^{-1})\;\Gamma\,(\text{mol cm}^{-2}) \quad (11)$$

where the units of the various quantities are given in parentheses. Note that since this effective heterogeneous rate constant has units of cm s^{-1}, it can be directly compared to the heterogeneous collision frequency of ca. 10^4 cm s^{-1} (17,18), which represents the value of the largest heterogeneous rate constant that can be measured (i.e. the interfacial diffusion controlled rate constant). Taking a reasonable value for an experimentally tractable surface coverage of 10^{-10} mol cm^{-2}, one predicts that the maximum value of k_{crs} which can be measured by these methods is near the homogeneous diffusion controlled limit of ca. 10^{11} M^{-1} s^{-1}. Given this rate constant, Equation 6 predicts a shift of the mediated wave of ca. 400 mV, which represents the maximum possible potential shift. On the other hand, measurement of very low rate constants (e.g. below 10^3 M^{-1} s^{-1}) will be difficult due to the very small *shifts in the peak potential* of the mediated wave from the formal potential of the redox catalyst within the SAM.

It is remarkable that these considerations predict that second order rate constants approaching the diffusion controlled value can be measured by this method, especially given the level of difficulty usually associated with measurement of such rapid processes. A significant factor contributing to this conclusion is that large currents need not be passed to measure these large rate constants. Usually, electrochemical measurement of large heterogeneous electron transfer rate constants is accomplished with rapid potential perturbations (fast scan rates, potential steps, high frequencies, etc.) which frequently lead to large currents and all of the experimental problems associated with large current measurements (such as resistive potential drops (22)). In contrast, the present method generates the kinetic information by virtue of a large potential shift. Thus, since large currents need not be passed, the associated experimental problems are alleviated. However, there are several caveats to these conclusions. First, the rate constant for the inner electron

exchange process between the immobilized redox group and the electrode, k_S, must be sufficiently fast so that it does not present kinetic limitations of its own. Given the relative scarcity of quantitative information on rate constants for immobilized redox species, it is difficult to make generalizations about this point. Second, the monolayer structure containing one of the partners in the cross reaction must present an effective barrier for the solution phase redox reagent, even under conditions of the extremely large driving forces which will be required to generate these large rate constants. In other words, when the electrode overpotential is sufficiently large, the solution phase reagent may be oxidized or reduced simply by tunneling directly through the SAM, without the benefit of mediation by the immobilized redox group. These two factors will probably provide upper limits on the values of rate constants that can be measured by the method described in this study, however, in the absence of more quantitative information on these processes it is difficult to make predictions of these upper limits.

The fact that the Marcus model works as well as it does in the present case, given the distance dependence correction discussed above, suggests that the **intrinsic** barrier for the cross reaction is not too different in the SAM than it is in solution. For the V^+ and $Ru(NH_3)_6^{3+}$ reaction partners, this barrier is likely to be dominated by the outer sphere reorganization energy, λ_O, which is influenced by the medium through the static (D_S) and optical dielectric (D_{Op}) constants (where λ_O is proportional to $(1/D_{Op} - 1/D_S)$ (18)). In the present case, the change in medium from solution to the interior of the SAM does not seem to have much influence on the distance corrected rate constant, probably due to the dominance of $1/D_{Op}$ over $1/D_S$. This is expected for relatively polar media, where the D_{Op} values are much smaller than the D_S values. These considerations suggest that, while the intrinsic electron transfer reactivity of molecules within monolayer structures is relatively unaffected by the medium, the overall rates of reaction may be very different due to the influence of the structural features of the monolayer assembly, such as steric congestion, distance effects, etc. This finding lends strong support to the continuation of studies of the structural features of these assemblies, since they seem to constitute the primary way in which the reactivity of interfacial species can be manipulated.

Acknowledgement

We are grateful to the Office of Naval Research for the full support of this work. Thanks are due to Dr. Hugh De Long for initiating our studies in electron mediation.

References

1. Ulman,A. "An Introduction to Ultrathin Organic Films: from Langmuir-Blodgett to Self Assembly"; Academic Press: Boston, 1991.

2. Chidsey,C.E.D. *Science* **1992**, *251*, 919-922.

3. Finklea,H.O.; Hanshew,D.D. *J.Am.Chem.Soc.* **1992**, *114*, 3173-3181.

4. Moser,C.C.; Keske,J.M.; Warncke,K.; Farid,R.S.; Dutton,P.L. *Nature* **1992**, *355*, 796-802.

5. DeLong,H.C.; Buttry,D.A. *Langmuir* **1990**, *6*, 1319-1322.

6. DeLong,H.C.; Buttry,D.A. *Langmuir* **1992**, *8*, 2491-2496.

7. Goss,C.A.; Charych,D.H.; Majda,M. *Anal.Chem.* **1991**, *63*, 85-88.

8. Rodriguez,J.F.; Mebrahtu,T.; Soriaga,M.P. *J.Electroanal.Chem.* **1987**, *233*, 283-289.

9. Buttry,D.A.; Ward,M.D. *Chem.Rev.* **1992**, *92*, 1355-1379.

10. Tang,X.; Schneider,T.; Buttry,D.A., submitted to *Langmuir*.

11. a) Ikeda,T.; Leidner,C.R.; Murray,R.W. *J.Am.Chem.Soc.* **1981**, *103*, 7422-7425. b) Anson, F.C. *J. Phys. Chem.* **1980**, *84*, 3336-42.

12. Saveant,J.M. *J.Phys.Chem.* **1988**, *92*, 1011-1013.

13. Hong,H.-G.; Mallouk,T.E. *Langmuir* **1991**, *7*, 2362-2369.

14. Laviron,E. *J.Electroanal.Chem.* **1979**, *101*,19-28.

15. Finklea,H.O.; Avery,S.; Lynch,M.; Furtsch,T. *Langmuir* **1987**, *3*, 409-413.

16. Rocklin,R.D.; Murray,R.W. *J.Phys.Chem.* **1981**, *85*, 2104-2112.

17. Andrieux,C.P.; Saveant,J.M. *J.Electroanal.Chem.* **1978**, *93*, 163-168.

18. Marcus, R.M.; Siddarth, P. In "Photoprocesses in Transition Metal Complexes, Biosystems, and Other Molecules", Kochanski, E., Ed.; Kluwer Academic Publishers: Amsterdam, Netherlands; 1992, pp. 49-88.

19. Taube, H. *Adv. Chem. Ser., No. 162*, **1977**, 127-53.

20. Bock,C.R.; Connor,J.A.; Gutierrez,A.; Meyer,T.J.; Whitten,D.G.; Sullivan,B.P.; Nagle,J.K. *Chem.Phys.Lett.* **1979**, *61*, 522-525.

21. Li, J.; Kaifer, A.E. *Langmuir* **1993**, *9*, 591-96.

22. Barr,S.W.; Guyer,K.L.; Li, T.T.-T.; Liu,H.Y.; Weaver,M.J. *J.Electrochem.Soc.* **1984**, *131*, 1626-1631.

23. This range of distances is obtained from a variety of calculations of the $-CH_3$ group diameter including summation of van der Waals radii for C (1.5 Å) and H (1.2 Å) plus the C-H bond length (1.1 Å) giving a diameter of 3.8 Å, calculating the area per molecule for Langmuir-Blodgett monolayers (18 $Å^2$/molecule) giving a diameter of an alkyl chain of 4.8 Å, and estimation from molecular models giving a diameter of ca. 4.5 Å.

24. Creager, S.E.; Collard, D.M.; Fox, M.A. *Langmuir* **1990**, *6*, 1617-20.

Figure Captions

1. Schematic of the kinetic situation at the electrode/SAM/solution interface, where n and m represent the number of methylenes in the inner and outer alkyl chains, respectively, A^- is the charge compensating anion within the SAM (see text), and Ox and Red are $Ru(NH_3)_6^{3+}$ and $Ru(NH_3)_6^{2+}$, respectively.

2. CV scans of a 1V110SH monolayer with $\Gamma \approx 0.87 \times 10^{-10}$ mol cm^{-2} in 0.1 M NaCl at scan rates of 1 V s^{-1} (upper curve) and 25.6 V s^{-1} (lower curve).

3. Plot of $E_{p,a}$ (upper curve) and $E_{p,c}$ (lower curve) versus log scan rate (in V s^{-1}) for the 1V10SH monolayer shown in Figure 2.

4. CV scans for a) 1V10SH monolayer in 0.1 M NaCl with $\Gamma = 3.3 \times 10^{-10}$ mol cm^{-2} at a scan rate = 100 mV s^{-1}, b) the same monolayer in 0.1 M NaCl + 0.5 mM $Ru(NH_3)_6Cl_3$ at a scan rate = 50 mV s^{-1}, and c) 2.0 mM $Ru(NH_3)_6Cl_3$ at a bare electrode in 0.1 M NaCl at a scan rate of 10 mV s^{-1}.

5. Plot of $1/i_{obs,p}$ vs. $1/[Ru(NH_3)_6^{3+}]$ for a 1V16SH monolayer with $\Gamma = 3.3 \times 10^{-10}$ mol cm^{-2} under the same conditions as in Figure 4b, except for changing $[Ru(NH_3)_6^{3+}]$.

6. CV (left) and EQCM (right) scans for a 1V16SH monolayer with $\Gamma = 3.3 \times 10^{-10}$ mol cm^{-2} in 0.1 M NaCl A) scan rate = 200 mV s^{-1}, B) scan rate = 100 mV s^{-1} and $[Ru(NH_3)_6Cl_3]$ = 0.5 mM, C) scan rate = 100 mV s^{-1} and $[Ru(NH_3)_6Cl_3]$ = 30 mM.

SCHEME 1

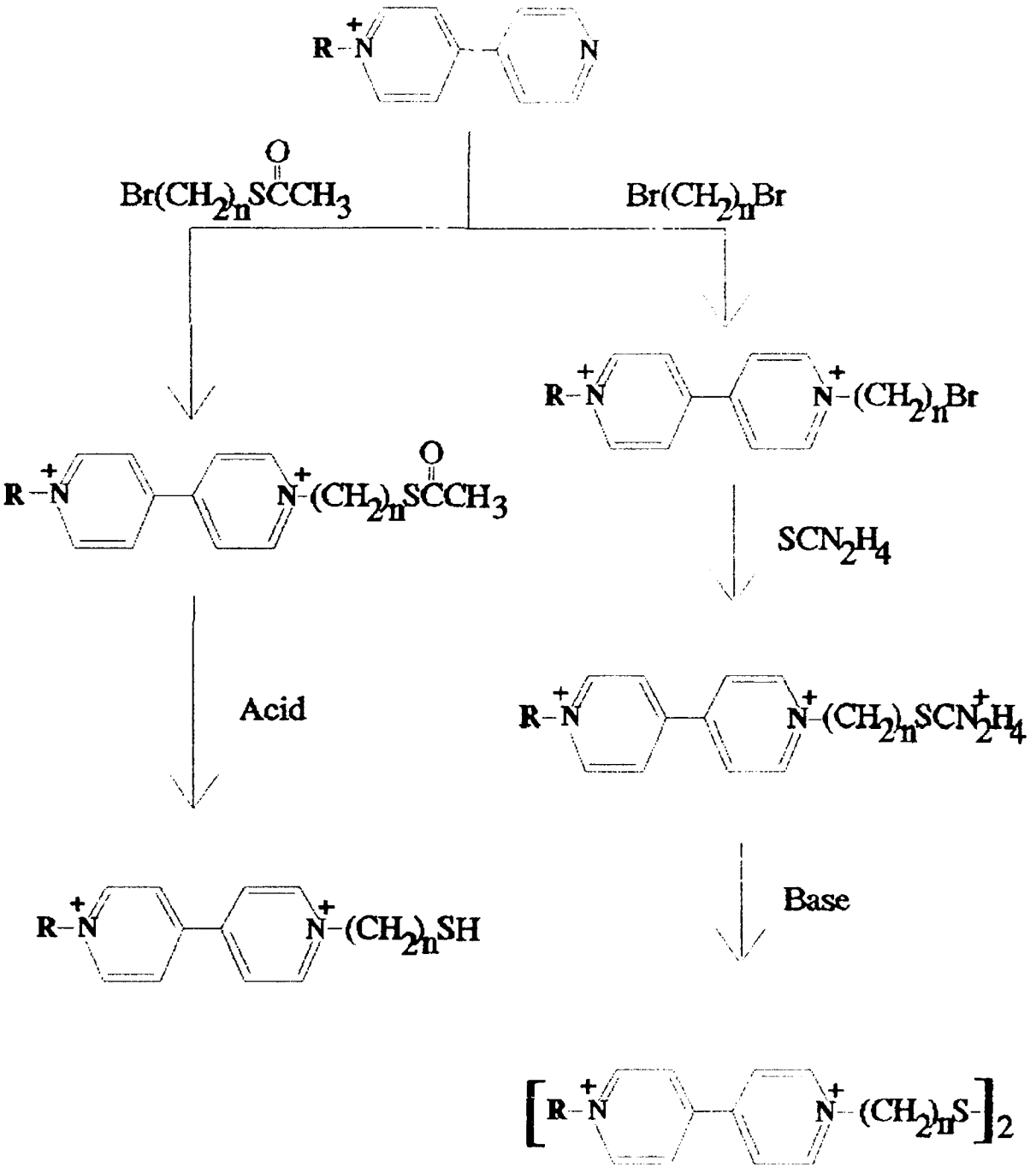

Scheme 1

TABLE 1

ANODIC AND CATHODIC k_S AND TRANSFER COEFFICIENT VALUES FOR METHYL TERMINATED VIOLOGEN SAM'S

	Γ (moles/cm^2)	α	1 - α	$k_{s,c}$ /s^{-1}	$k_{s,a}$ /s^{-1}
1V10SH	0.87×10^{-10}	0.23	0.18	62	60
1V12SH	0.18×10^{-10}	0.17	0.13	37	28
1V16SH	1.29×10^{-10}	0.24	0.24	9.2	6.3

TABLE 2

FORMAL POTENTIALS, MEDIATED PEAK SHIFTS, AND CROSS REACTION RATE CONSTANTS FOR VIOLOGEN SAM'S REACTING WITH $Ru(NH_3)_6^{3+}$

	Γ moles/cm^2	$E^1/_2$ (V)	$^*E_{p,c}$ (V)	k_{crs} $M^{-1}s^{-1}$
1V10SH	3.3×10^{-10}	-0.43	-0.39	6.0×10^4
1V12SH	2.6×10^{-10}	-0.45	-0.40	11×10^4
1V16SH	3.3×10^{-10}	-0.47	-0.42	8.0×10^4
$[10V10S]_2$	3.4×10^{-10}	-0.38	-0.37	2.2×10^4
$[ChoV5S]_2$	1.3×10^{-10}	-0.49	-0.44	25×10^4
$[F10H2V5S]_2$	3.3×10^{-10}	-0.32	-0.32	1.5×10^4

Figure Captions

1. Schematic of the kinetic situation at the electrode/SAM/solution interface, where n and m represent the number of methylenes in the inner and outer alkyl chains, respectively, A^- is the charge compensating anion within the SAM (see text), and Ox and Red are $Ru(NH_3)_6^{3+}$ and $Ru(NH_3)_6^{2+}$, respectively.

2. CV scans of a 1V 10SH monolayer with $\Gamma = 0.87 \times 10^{-10}$ mol cm^{-2} in 0.1 M NaCl at scan rates of 1 V s^{-1} (upper curve) and 25.6 V s^{-1} (lower curve).

3. Plot of $E_{p,a}$ (upper curve) and $E_{p,c}$ (lower curve) versus log scan rate (in V s^{-1}) for the 1V10SH monolayer shown in Figure 2.

4. CV scans for a) 1V10SH monolayer in 0.1 M NaCl with $\Gamma = 3.3 \times 10^{-10}$ mol cm^{-2} at a scan rate = 100 mV s^{-1}, b) the same monolayer in 0.1 M NaCl + 0.5 mM $Ru(NH_3)_6Cl_3$ at a scan rate = 50 mV s^{-1}, and c) 2.0 mM $Ru(NH_3)_6Cl_3$ at a bare electrode in 0.1 M NaCl at a scan rate of 10 mV s^{-1}.

5. Plot of $1/i_{obs,p}$ vs. $1/[Ru(NH_3)_6^{3+}]$ for a 1V16SH monolayer with $\Gamma = 3.3 \times 10^{-10}$ mol cm^{-2} under the same conditions as in Figure 4b, except for changing $[Ru(NH_3)_6^{3+}]$.

6. CV (left) and EQCM (right) scans for a 1V16SH monolayer with $\Gamma = 3.3 \times 10^{-10}$ mol cm^{-2} in 0.1 M NaCl A) scan rate = 200 mV s^{-1}, B) scan rate = 100 mV s^{-1} and $[Ru(NH_3)_6Cl_3] = 0.5$ mM, C) scan rate = 100 mV s^{-1} and $[Ru(NH_3)_6Cl_3] = 30$ mM.

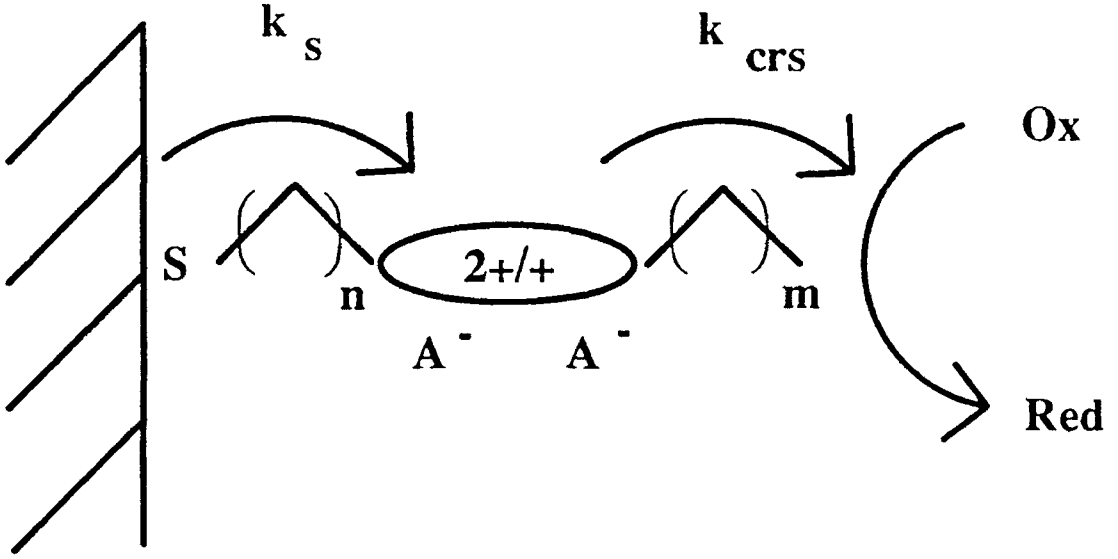
k s
k crs
Ox
S
n
2+/+
m
A -
A -
Red

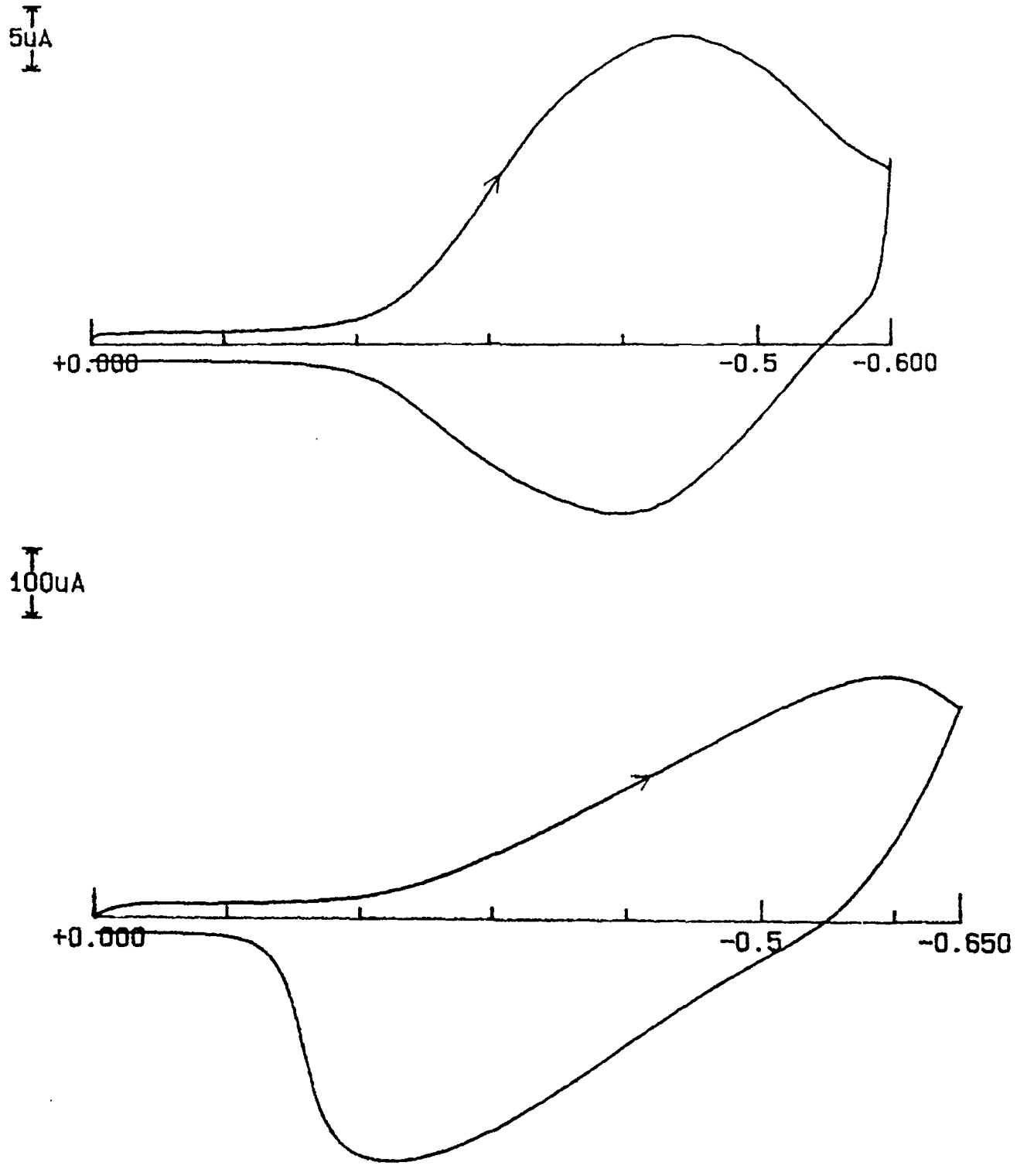
5uA
+0.000
-0.5
-0.600
100uA
+0.000
-0.5
-0.650
E (VOLT)

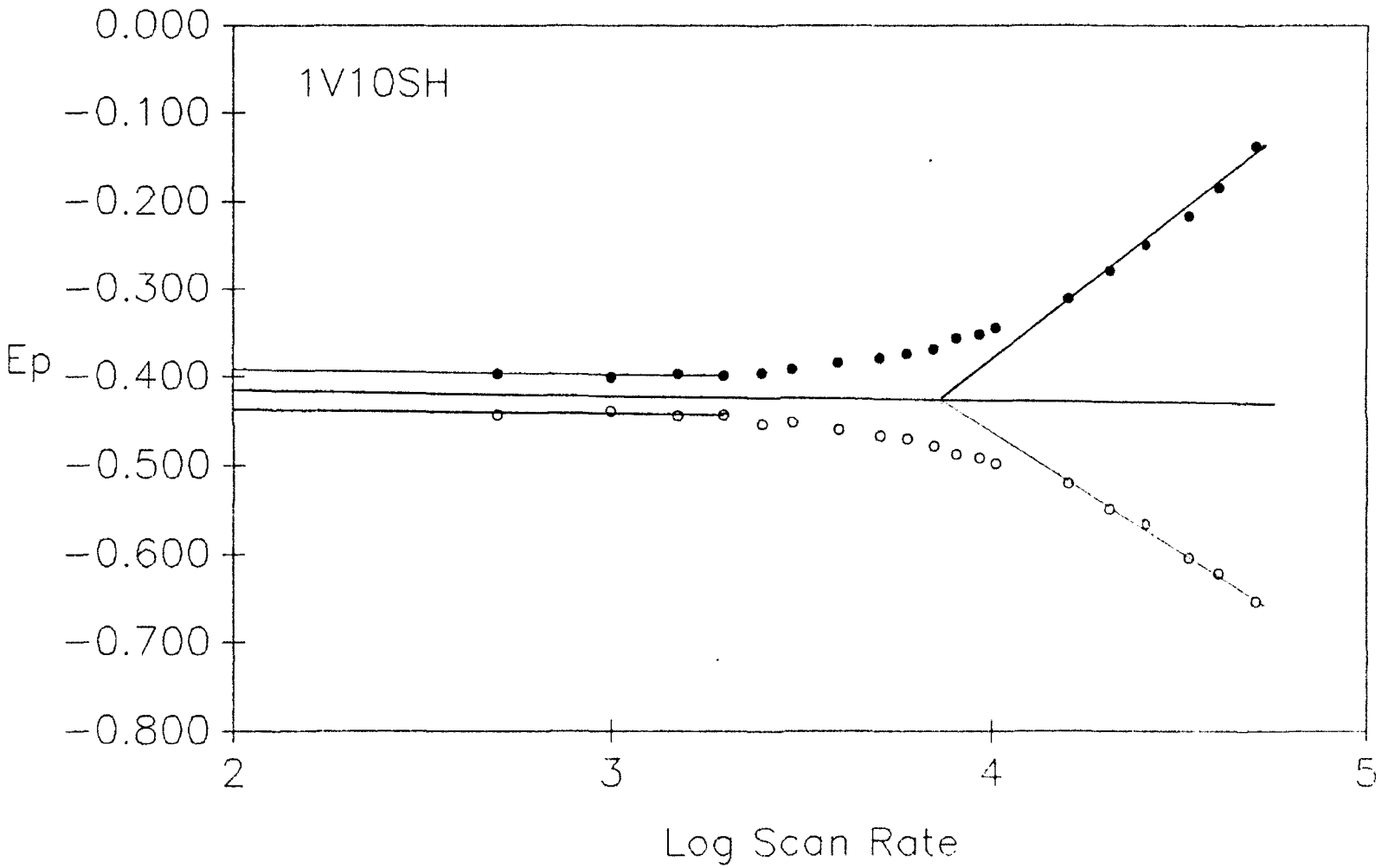
1V10SH
0.000
-0.100
-0.200
-0.300
-0.400
-0.500
-0.600
-0.700
-0.800
Ep
2
3
4
5
Log Scan Rate

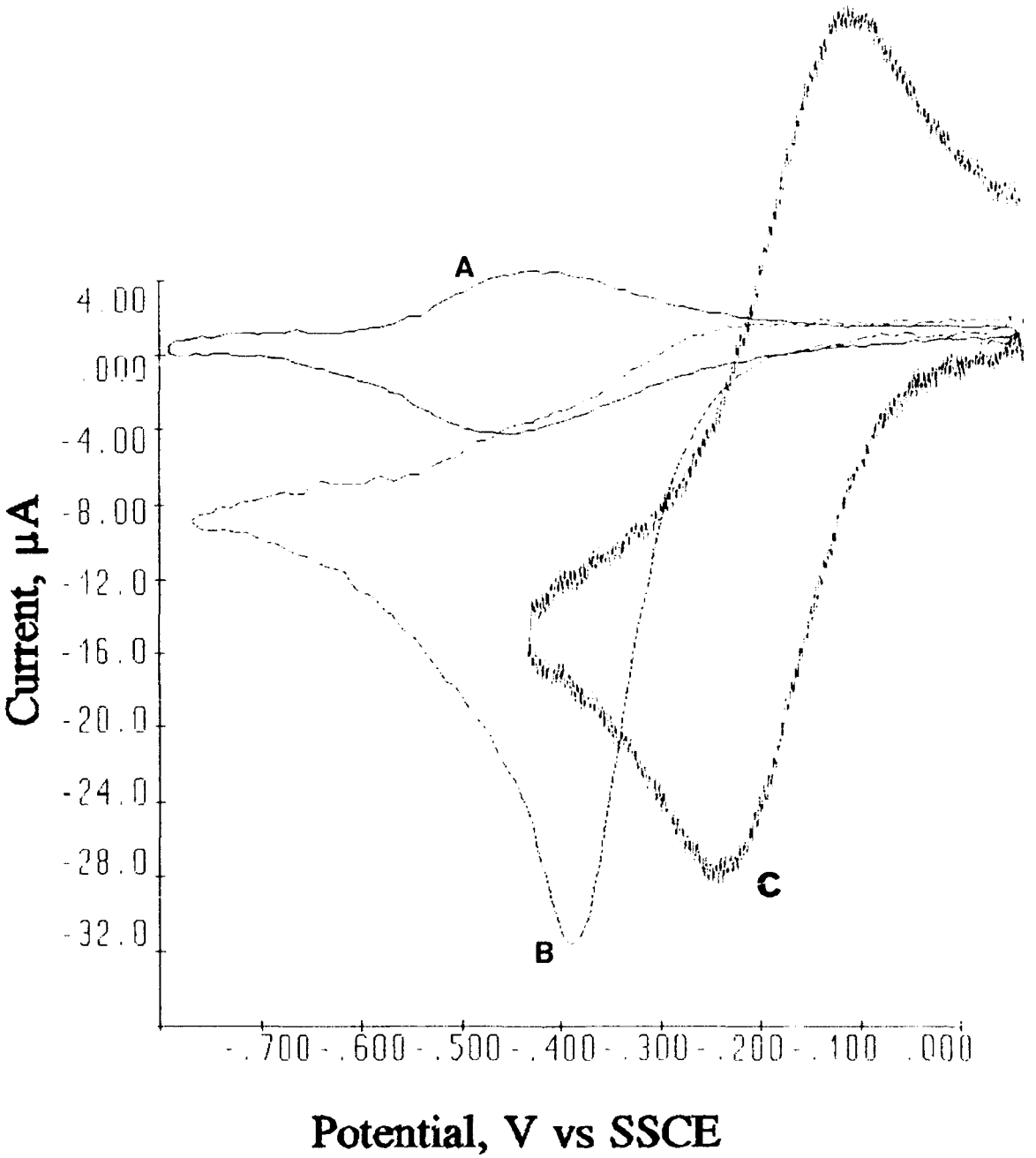
A
B
C
4.00
.000
-4.00
-8.00
-12.0
-16.0
-20.0
-24.0
-28.0
-32.0
Current, µA
-.700 -.600 -.500 -.400 -.300 -.200 -.100 .000
Potential, V vs SSCE

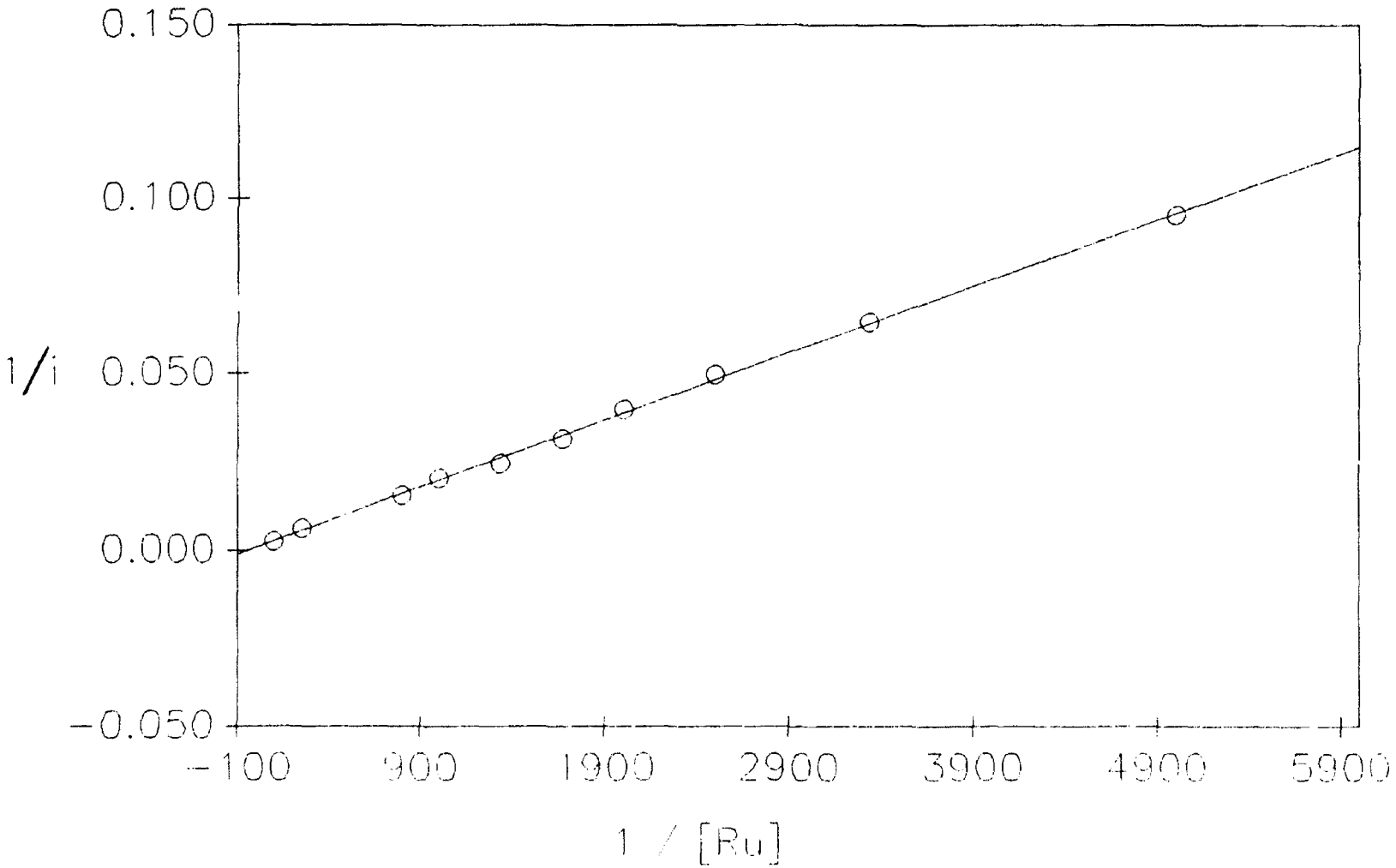
0.150
0.100
1/i
0.050
0.000
-0.050
-100
900
1900
2900
3900
4900
5900
1 / [Ru]

A.

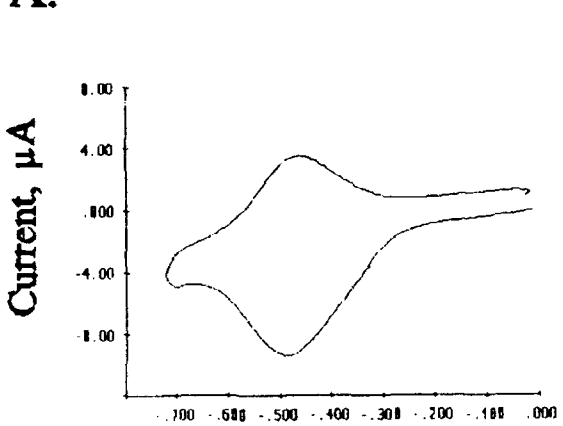

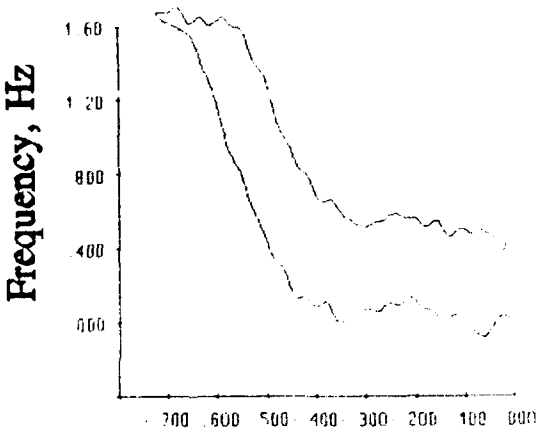

B.

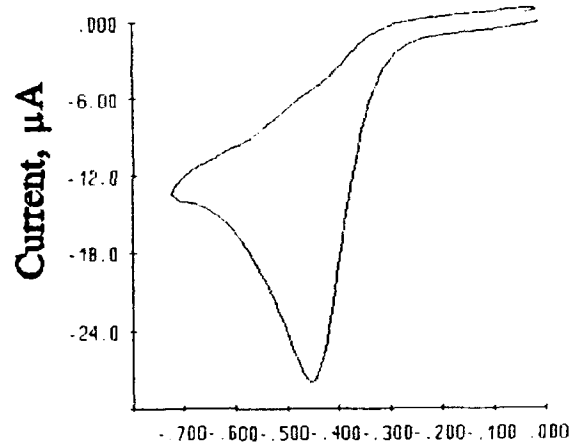

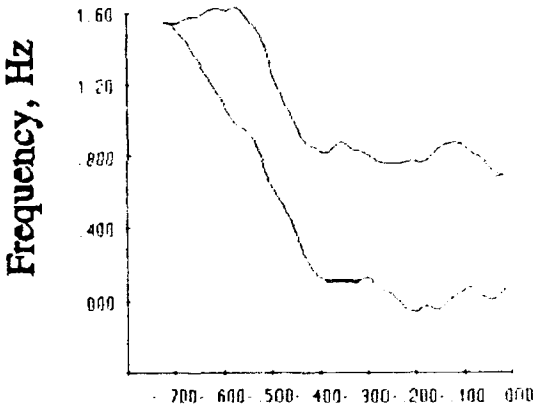

C.

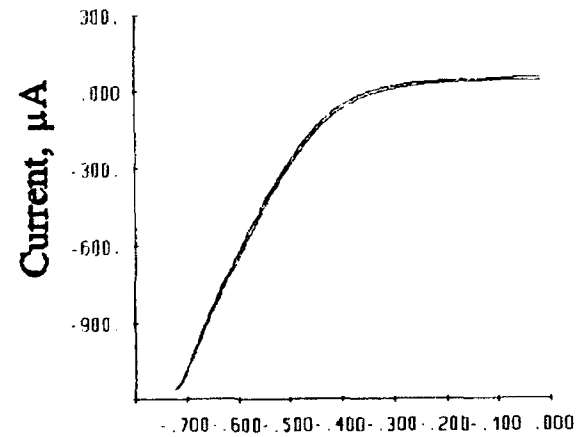

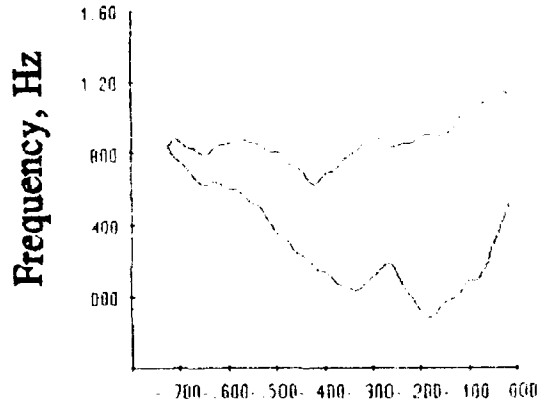

Potential, V vs SSCE

Potential, V vs SSCE